Pergamon

0301-9322(94)00088-3

Int. J. Multiphase Flow Vol. 21, No. 4, pp. 569–589, 1995

0301-9322/95 $9.50 + 0.00

GAS–LIQUID ANNULAR FLOW AT A VERTICAL TEE JUNCTION—PART I. FLOW SEPARATION

Y. CHARRON[1] and P. B. WHALLEY[2]

[1]Total, 24 Cours Michelet, 92069 Paris la Defense, France
[2]University of Oxford, Department of Engineering Science, Oxford, England

(Received 8 August 1994; in revised form 22 November 1994)

Abstract—Some mechanisms of flow separation at a vertical tee junction with a horizontal outlet are examined in single-phase and two-phase annular flows. In single-phase flow, some characteristics of the vena contracta at the vertical exit and the shape of the dividing streamline boundaries at the tee entrance are measured. In two-phase flow, experiments carried out with cotton threads indicate, that at low branch take-off a large fraction of the liquid film flow entering the branch is rejected to the tee then entrained to the vertical exit. At high branch take-off, some of the liquid in the vertical exit falls back into the tee junction. This phenomenon is examined with a liquid dye and a high speed video camera, indicating two causes for the liquid to fall along this tube and providing some information on the subsequent division of the falling flow. Finally, the predictions of several flow separation models are compared with the present data and the validity of some assumptions made in mechanistic models is reviewed in relation with the observations provided by the present experiments.

Key Words: annular flow, tee junction, flow separation, velocity profiles

1. INTRODUCTION

The simultaneous flow of two phases occurs widely in industrial applications: oil and gas pipelines, gas condensation during gas transport, oil field steam injection, nuclear plants, distillation columns, steam generators or heat exchangers. The liquid and gas interface can present very different shapes (patterns) according to the phase flowrates, the flow direction or physical parameters like surface tension or viscosity. The flow direction is an important parameter. It makes the flow asymmetric in horizontal channels, causes counter current flows in vertical channels, conditioning the degree of phase separation at a branching junction.

A particular flow pattern of interest is annular flow as it is encountered in many applications and occurs over a wide range of flow conditions. Many sub-divisions of annular flow may be considered: *annular–rivulet* flow is produced at an extremely low liquid flowrate. Slightly increasing the liquid flowrate produces a pure *annular* flow with a continuous liquid film around the channel wall and no liquid phase in the gas core. When the liquid flowrate exceeds a critical film flowrate, the liquid is partially entrained in the gas core and an *annular–mist* flow is obtained. At higher liquid flowrates, large lumps or wisps appear in the gas core, producing *wispy–annular* flow. If the gas flowrate is reduced at a low or medium liquid flowrate, *churn–annular* flow may be obtained in vertical channels and *semi-annular* flow in horizontal channels.

Pipe junctions are commonly used in single-phase flow, but in two-phase flow they are usually avoided where possible. Sometimes junctions are used because they act as partial phase separators. Examples of two-phase junctions include slug catchers and wet steam injection manifolds for enhanced oil recovery; there is also the case of a pipe rupture in a nuclear reactor during a loss of coolant accident (LOCA). It is mainly during the last two decades that the increasing number of two-phase flow applications has intensified the research in branching junctions. Studies have been mainly carried out to improve the knowledge of the phase division phenomenon in branching junctions and manifolds. These studies have shown the great complexity of analysing the separation phenomenon in the general case.

The present state of understanding of the two-phase flow separation has identified some of the important parameters: flow pattern (Azzopardi & Whalley 1982; Shoham & Brill 1987), gravity force (Azzopardi 1988; Reimann *et al.* 1988), liquid level in stratified flow (Maciaszek & Micaelli

1988), radial void distribution (Hervieu 1988), inlet diameter (Azzopardi 1992), flow viscosity (Hong 1978) and branch-inlet diameter ratio (Azzopardi 1984; Zetzmann 1982).

In annular–mist flow, three mechanisms of liquid entrainment to the side-branch are generally considered:

—part of the liquid film is directly entrained into the branch. This is determined by taking into account drag forces, centrifugal forces (Shoham & Brill 1987; Hwang *et al.* 1988), pressure forces (Ballyk & Shoukri 1990) or also surface tension forces (Sliwicki & Mikielewicz 1988). In the particular case of zero branch gas flowrate, Sliwicki predicts that a relatively high liquid film fraction is entrained to the branch (creeping flow). For very small inlet water flowrate, Azzopardi (1988) found that the fraction of liquid film entering the branch rapidly increases due to a pressure build up occurring at the straight through tee outlet above a certain gas branch take-off (film stop);
—some of liquid droplets carried by the high speed gas core may also be diverted to the side branch and be entrained into it (Hwang and Sliwicki);
—the gas flow into the vertical outlet may be insufficient to carry the liquid upwards. In these circumstances the liquid can fall back and enter the side tube (Azzopardi & Purvis 1987).

2. EXPERIMENTS

All the experiments described below have been performed in an apparatus consisting of acrylic resin transparent tubes, mounted vertically, air and water supply systems with controls and metering. The test section had the following characteristics:

—internal diameter 32 mm and length 5 m;
—air and water flows were upward. The water flow entered through an axial injector at the bottom of the vertical test section, where it was mixed with air;
—tee junctions were mounted 2.9 m downstream the water injector.

The test conditions were the following:

—pressure controlled to 1.5 bar at the tee location. Temperature between 16 and 22°C;
—flowrates varied: air between 10 and 85 g/s, water between 3.5 and 78 g/s.

Before the tee junction was installed, experiments were carried out in a straight tube with a two-phase flow in order to:

(a) measure at the tee location, the liquid film fraction (using a circumferential porous sinter), and the radial profiles of the gas velocity and the water droplet flowrate (using a sampling probe);
(b) evaluate the degree of flow equilibrium at the tee location, by also measuring the liquid film fraction 1 m upstream from the tee location and the pressure gradient along the test tube;
(c) ascertain the verticality of the test tube and the axial symmetry of the flow. This was performed by measuring the circumferential distribution of the liquid film flowrate (using a narrow window porous sinter) and the radial distribution of the droplet flowrate.

Only some of the sampling probe results are presented in this paper. The liquid film fraction and pressure gradient results are not presented here but may be found in Charron (1993).

2.1. Profiles of gas velocity and liquid droplet flowrate at a tube cross section

Gill *et al.* (1963) carried out profile measurements for gas velocity and liquid droplet flowrate in a vertical tube for air flowrate varying from 25 to 88 g/s and water flowrate varying from 4 to 125 g/s. These measurements were taken 5.3 m downstream from a radial type water injector (porous sinter), in a 32 mm diameter tube. In the present case, knowledge of the profile characteristics is required at the tee junction level, i.e. 2.9 m only downstream from the air–water mixing while the water injector is of the axial type. The Gill data are therefore not fully applicable

to the present case. Adorni (1961) and Schraub (1966) also performed sampling probe experiments but for fluid and flow conditions considerably different to the present ones.

In the present study, the profiles are established with the sampling probe outlet closed (and therefore acting as a Pitot tube) for the gas velocity and the sampling probe set to isokinetic conditions for the droplet flowrate.

2.1.1. Gas velocity profiles. According to Gill, the gas velocity, U_G, can be deduced from the measured impact pressure, ΔP_i, from:

$$\Delta P_i = \tfrac{1}{2}\rho_h U_G^2 \quad [1]$$

assuming a homogeneous flow at the probe inlet. Adorni taking into account, in a momentum balance equation, the progressive phase separation occurring in front of the probe tip, suggested:

$$\Delta P_i = \tfrac{1}{2}(\epsilon^2 \rho_G U_G^2 + (1-\epsilon^2)\rho_L U_L^2) \quad [2]$$

In these equations, ϵ is the void fraction; ρ_G, ρ_L, U_G and U_L are the gas and liquid densities and actual velocities; ρ_h is the homogeneous density. Schraub modified the Adorni equation by assuming that the gas–droplet velocity ratio varies as the mixture decelerates from the free stream value far from the probe tip to unity where the void fraction becomes zero. However the effect of this modification is minor in the present case as the Adorni and Schraub equations provide approximately the same results.

The suitability of the above equations was evaluated at different flow conditions by integrating the local gas velocities over three tube traverses (at 60° intervals) and by comparing the resulting flowrate with the measured inlet flowrate. The deviation was smallest using the Adorni equation and generally less than 5% (except in the churn–annular flow transition where it once reached 10%) whereas it was frequently above 10% using the homogeneous equation.

Examples of gas velocity profiles are plotted in figure 1 for a water flowrate of 63 g/s. A comparison between the different inlet flow conditions indicates that the velocity profile is more peaked when the quality is small (the air flowrate low or the water flowrate high). The same trend was also observed by Gill who attributed this effect either to the suppression of turbulent eddies

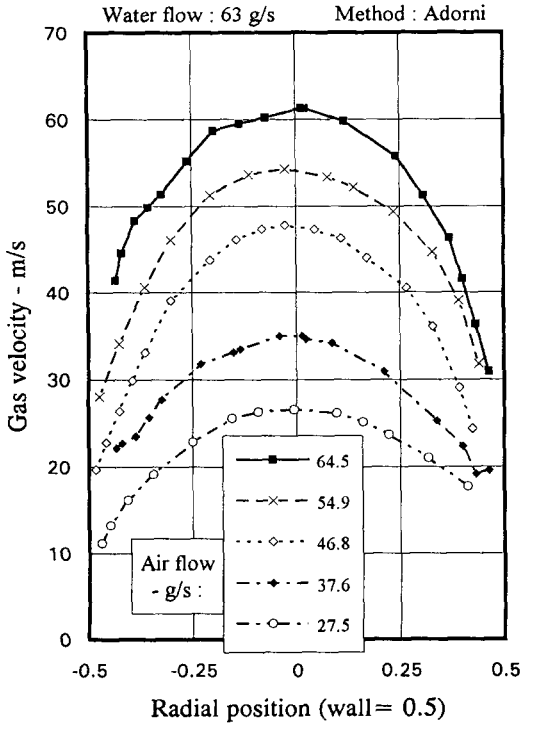

Figure 1. Gas velocity profiles in two-phase flow. Pitot tube experiments.

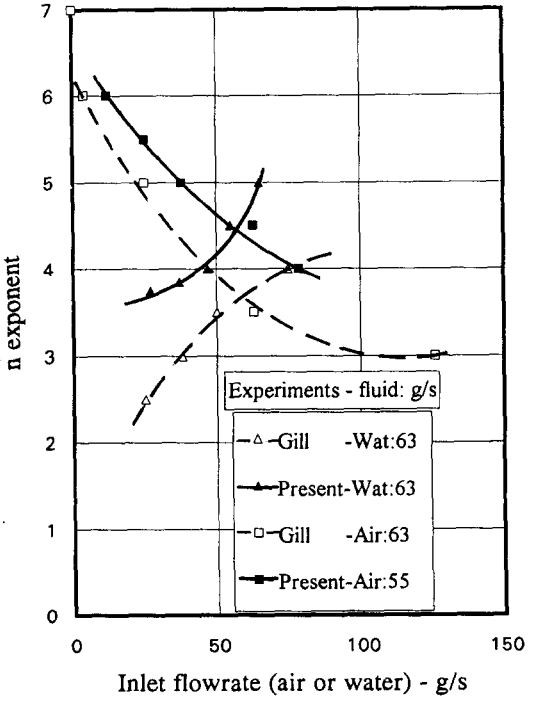

Figure 2. n exponent versus inlet air and water flowrates.

by the entrained droplets or to the large disturbance waves which are formed at high liquid flowrates. The second explanation seems to be more likely, particularly at low inlet gas flowrates where the entrained liquid flow is relatively limited.

These gas velocity profiles can be roughly represented by the following equation:

$$U = U_c(y/r_o)^{1/n} \quad [3]$$

where U is the velocity at a distance y from the tube wall, U_c the velocity at the tube centre, r_o the tube radius and n is a parameter. The values of n are shown in figure 2 together with the values from the Gill experiments. From this figure two observations can be made: firstly, the value of n reduces with the flow quality, secondly, the values found here are always greater than in the Gill case. This difference in results may be explained by considering the differences in the test conditions (the type of water injector and the distance between the injector and the measuring location). The liquid film thickness and flowrate being larger in the Gill case, it is possible that the disturbance waves have a stronger effect at the measuring location in the Gill case, causing a more peaked velocity profile.

2.1.2. Liquid droplet flowrate profiles. The local droplet flowrates were calculated from the sampling probe results when operating at isokinetic conditions, as described by Rao & Dukler (1971). An example of droplet flowrate profiles along one tube transverse is provided in figure 3 for a 63 g/s inlet water flowrate. At low air flowrates, the profiles present a "bowl" shape due to the probe occasionally catching some liquid from the large amplitude film waves (approximately 5 times the film thickness) when near the tube wall. As the inlet air flowrate increases, the profiles become flatter, only falling at 4 or 5 mm from the tube wall.

The data plotted in figure 3 were obtained after the vertical alignment of the test tube was achieved, represented here by configuration "c". During the course of the alignment, two other sets of data were recorded for misalignment angles of 0.08° (4 mm offset over a 2.9 m length) in two opposite directions. These two configurations are designated "a" and "b". Contours of constant droplet flowrates are plotted for these three configurations in figure 4 showing the extreme sensitivity of the radial droplet flowrate distribution to the test tube verticality.

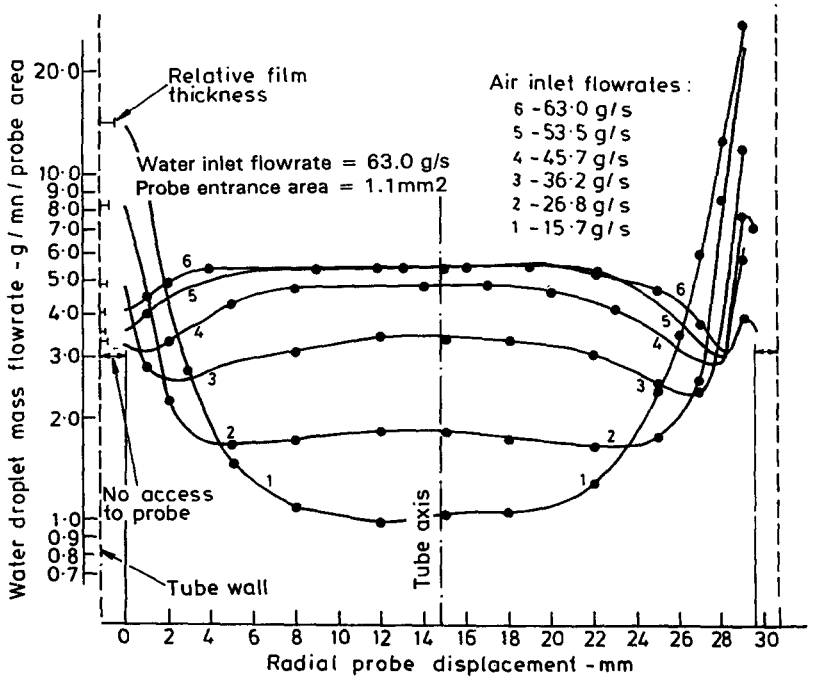

Figure 3. Water drop flowrate profiles for various air inlet flowrates.

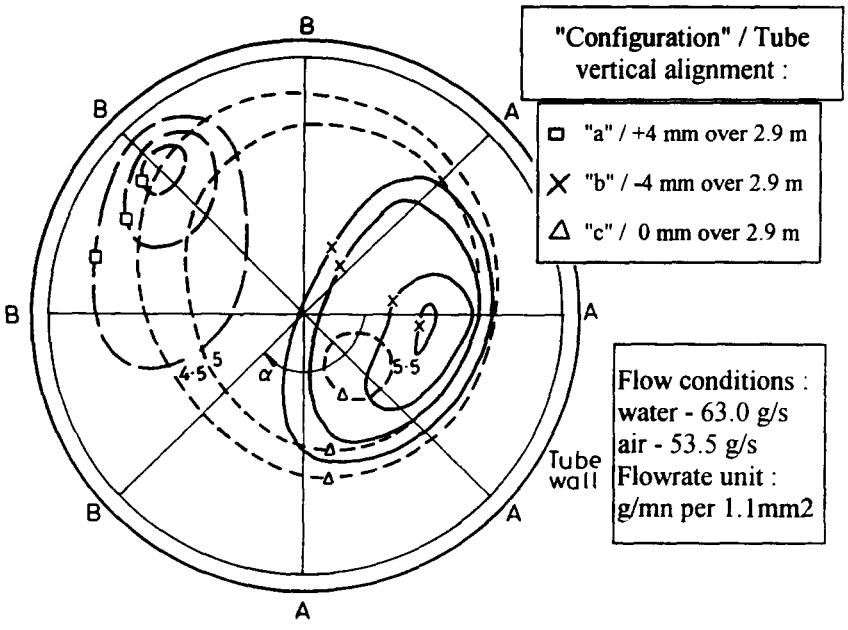

Figure 4. Water droplet flowrate distribution for various tube vertical alignments.

2.2. Gas separation at a tee junction in single-phase flow

In single-phase flow, the shape of the dividing streamline boundary affects the split of the kinetic energy between the tee outlets (this subject will be discussed in a subsequent paper). In modelling of two-phase flow, authors usually assume that the inlet fluid turning into the side-branch comes from a circular segment. The purpose of this experiment is two-fold: to provide data for an energy balance and to test the assumption that the flow comes from a circular segment.

To track flow streamlines, various techniques have been used in the past: dye injection with a hypodermic needle in water [Escobar (discussing the McNown paper) 1954]; cotton threads in

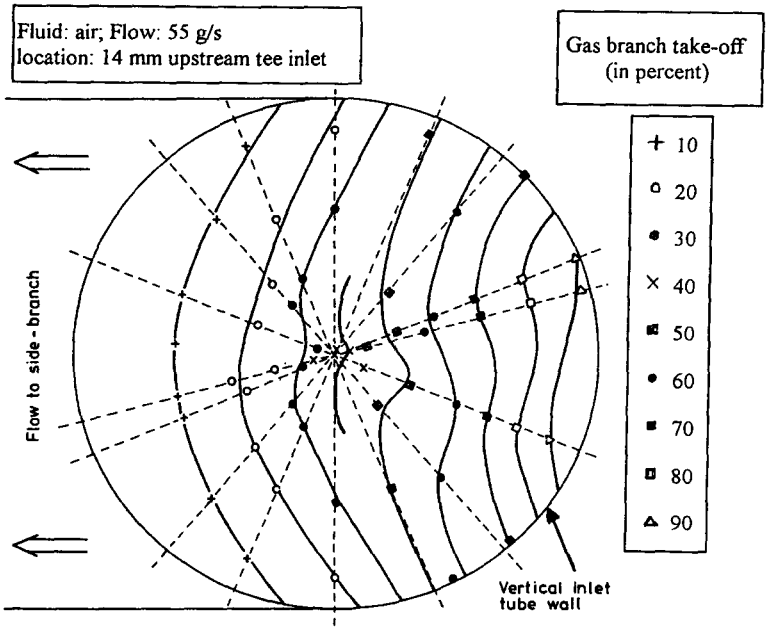

Figure 5. Dividing streamline boundaries at a tee junction inlet, in single-phase flow and for various flow splits.

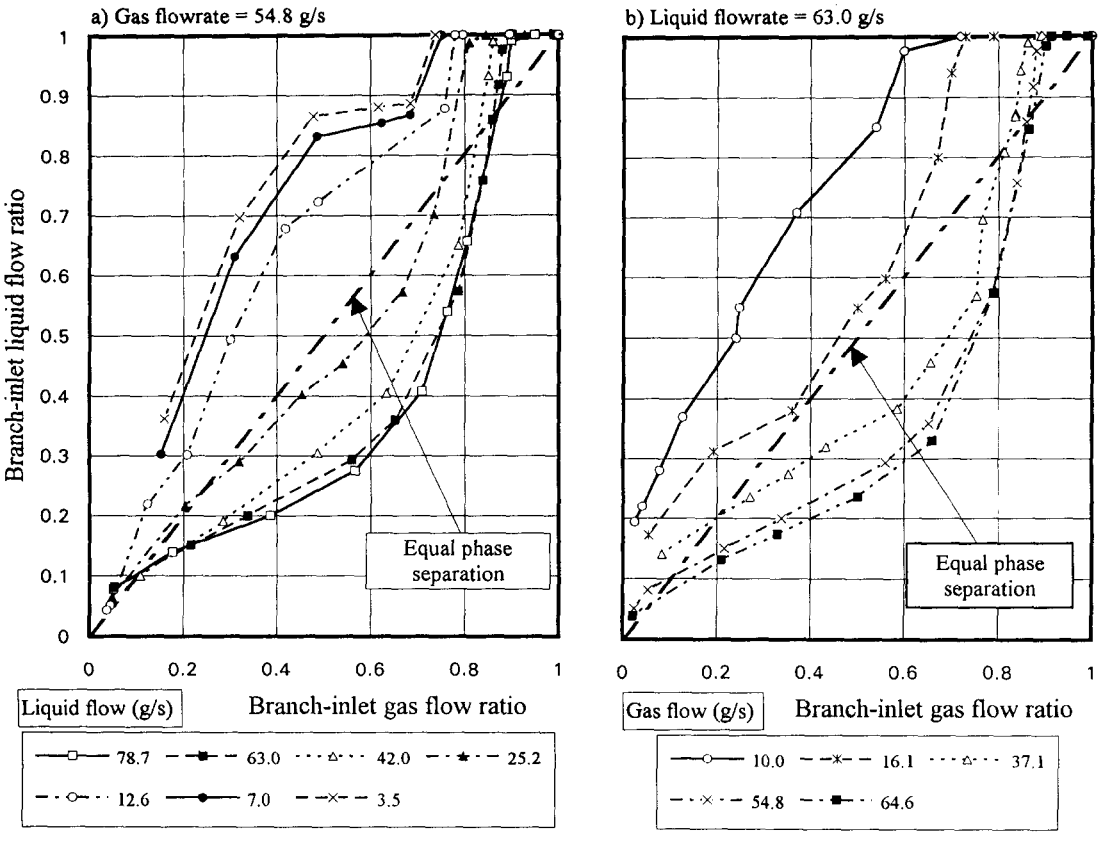

Figure 6. Liquid–gas phase relative separtion at a tee junction.

a gas flow (McCreery 1990) and lasers measuring particle characteristics: bubbles in a liquid phase (Hervieu 1988) or liquid droplets in a gas phase and in a straight pipe (Teixeira 1988).

In the present study, poor results were obtained with a liquid dye, due to rapid diffusion of the dye before the run–branch corner was reached. Streamlines could be identified relatively easily by using the cotton thread technique in conjunction with a tee originally designed for pressure measurements. This tee piece, an assembly of two tubes (0.5 m and 0.4 m long) mounted perpendicularly and provided with 1 mm diameter pressure tappings at intervals varying between 1 and 3 cm, was also found suitable for flow streamline visualization. It was used in the following manner: a cotton thread was attached to a 0.2 mm diameter metallic wire, inserted in a 0.8 mm external diameter hypodermic tube. Pulling the metallic wire could adjust the length of the cotton thread whereas moving the hypodermic tube in a tapping hole provided the required radial position. The location of a streamline was determined when the cotton thread ended at the run–branch corner. The air flowrate was set to 55 g/s. Measurements were taken for approximately twenty flow split cases and at three tube cross sections: 4, 14 and 24 mm below the tee entrance. Compiled boundary shapes established at the intermediate cross section are represented in figure 5.

2.3. Gas and liquid separation at a tee junction in two-phase flow

The tee piece for these experiments was made from a block of acrylic resin with the approximate dimensions 150 × 100 × 100 mm and bored (31.75 mm diameter) in two perpendicular directions with square edges at their intersection. The tubes attached to it, designated: inlet or main (2.9 m long); horizontal outlet or branch (2 m long) and vertical outlet or run (2 m long) were all transparent for flow visualization purposes.

The phase separation experiments were carried out at conditions similar to earlier ones by Azzopardi & Purvis (1987), except that: (a) the water entered the test tube axially instead of radially.

This is important because the flow equilibrium for the liquid film fraction is not reached after 2.9 m (see the note below); (b) the inlet water flowrate was varied down to 3.5 g/s; (c) pressure change and flow separation measurements were taken simultaneously to obtain a good match between

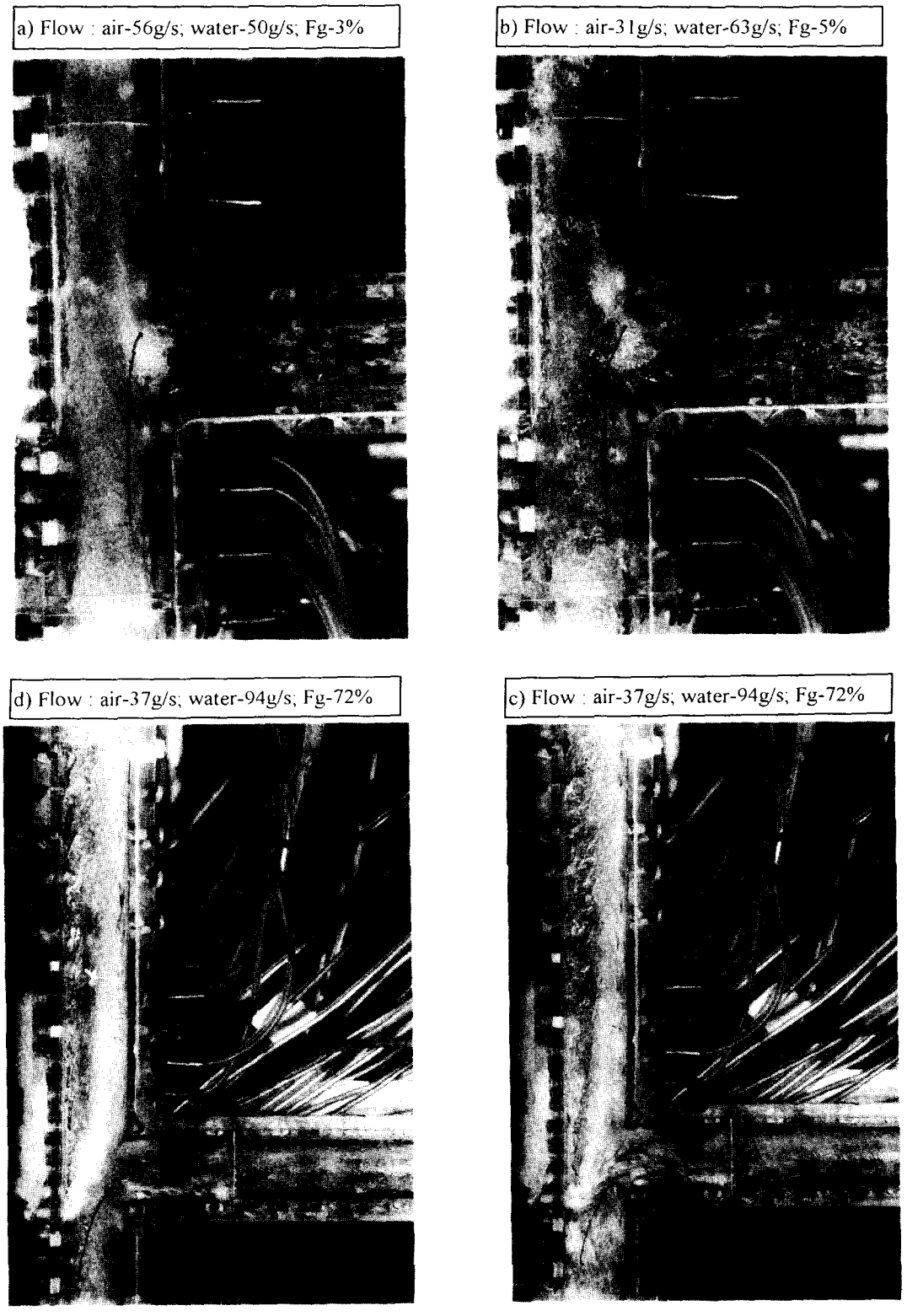

Figure 7. Flow separation at a vertical tee junction. Visual observations.

the two sets of data.† Some phase separation measurements are represented in figure 6(a) and (b). Some typical flow cases may be considered:

(1) Low water flowrate [figure 6(a)]. Phase separation occurs at the tee with the liquid preferentially flowing to the branch. This phenomenon is usually explained by considering the relatively low liquid entrainment in the gas core and the relatively high pressure gradient produced at the tee in the direction of the run, "stopping" the liquid film at the branch axis level where it is easily diverted to the side branch (Azzopardi 1988).

(2) High water, medium–high air flowrates [figure 6(b)]. This corresponds to an annular–mist flow at the tee inlet with most of the liquid phase carried by droplets flowing in the direction of the straight through tee outlet due to their relatively high momentum.

(3) Low air flowrate [figure 6(b)]. This corresponds to a churn flow at the tee inlet with most of the liquid phase flowing along the tube wall. Total phase separation is obtained when liquid flow reversal occurs at the run, caused by the dominant gravitational forces. The falling liquid is then easily removed by the horizontal side branch.

Two cases of liquid phase separation can be seen in figure 7:

photographs (a) and (b) representing the low gas branch take-off (F_G) case, characterized by a very thick liquid film layer at the bottom of the branch;

photographs (c) and (d) ($F_G = 72\%$). Liquid flow reversal occurs at the run, opposite the branch side. A liquid jet taking its source at the impact between the falling and rising liquid flows is mainly directed towards the run.

2.4. *Liquid film separation at a tee junction in two-phase flow*

When the gas branch take-off is not too large and when the location of the dividing streamline in the inlet liquid film is known, it is possible to compare the liquid film flowrate entering the side branch with the liquid flowrate leaving it, assuming that the liquid droplet flowrate entering the side-branch is negligible because of the relatively high momentum of the droplets.

The location of the film dividing the streamline was determined with a cotton thread, as in the single-phase air flow experiments. One end of the thread was fixed on the tube wall and then the flow split was adjusted until the other end settled at the run–branch corner. The hypodermic tube carrying the cotton thread was sufficiently far upstream of the tee entrance to ensure the flow was not already disturbed by the tee.

The validity of these experiments was assessed by ensuring that the liquid drag force applied on the cotton thread was sufficiently large in comparison with its weight. The results of the experiments were not dependable at low inlet flowrates: (a) below 25 g/s water flowrate, as the liquid film was too thin to drag the cotton thread, (b) below 25 g/s air flowrate, as the amplitude of the film flow fluctuations was too large to determine the position of the dividing streamline with sufficient accuracy.

2.5. *Flow behaviour at the vertical outlet*

In the past, some authors have studied the characteristics of the vena contracta at the run: Hervieu (1988) in bubbly flow; McCreery & Banerjee (1990) in mist flow. Measurements have been carried out here, both in single-phase and two-phase annular flows using different techniques and with the junction mounted vertically. All experiments were carried out with the tee used in section 2.2.

In single-phase flow, the occurrence and the length of the vena contracta at the run was determined successively with air, from cotton threads inserted at 1 cm intervals along the tube wall and opposite the branch line and with water, from a liquid dye injected at the same locations.

†The present experimental results for the phase separation at the tee junction are of general validity if one refers to the three fields (liquid film, liquid droplet and gas phase) immediately upstream of the tee junction. This is not the case however for the inlet liquid and gas phases as the experimental results vary with the distance separating the air–water mixing to the tee junction. Therefore, for given inlet gas and liquid flowrates, the knowledge of the liquid film fraction at the tee entrance (measured here) is sufficient to check the validity of existing models while the condition of flow equilibrium at the tee junction is not necessary.

Despite the difference in the fluids used and the techniques employed, the results were relatively similar. Results for the upper and lower limits of the vena contracta zone are shown in figure 8.

In two-phase flow, the region of the liquid falling along the vertical outlet was determined similarly to the previous case, except that only the liquid dye technique was used. Results are presented again in figure 8. In addition, high speed video films were taken at a speed of 1000 frames per second to analyse the behaviour of the falling liquid at the tee junction, that is, its re-injection into the vertical outlet or its entrainment to the branch. Photographs representing this situation are shown in figure 7 (photographs c and d).

2.6. Pressure measurements

Several experiments related to pressure measurements have also been carried out during the course of the present study. The results will be presented in a later paper. These experiments consisted of the measurement of:

—overall inlet–outlet pressure changes based on the extrapolation of pressure profiles
—local pressure changes, at closely spaced (1 cm) pressure tappings in the vicinity of the tee and round the tube periphery. The total number of tapping points was in the order of 200.

3. COMPARISON OF FLOW SEPARATION MODEL PREDICTIONS WITH PRESENT MEASUREMENTS

Many flow separation experiments at junctions (tees, wyes) have been carried out in the last two decades, with most of the works performed with a horizontal inlet. Only the work by Azzopardi

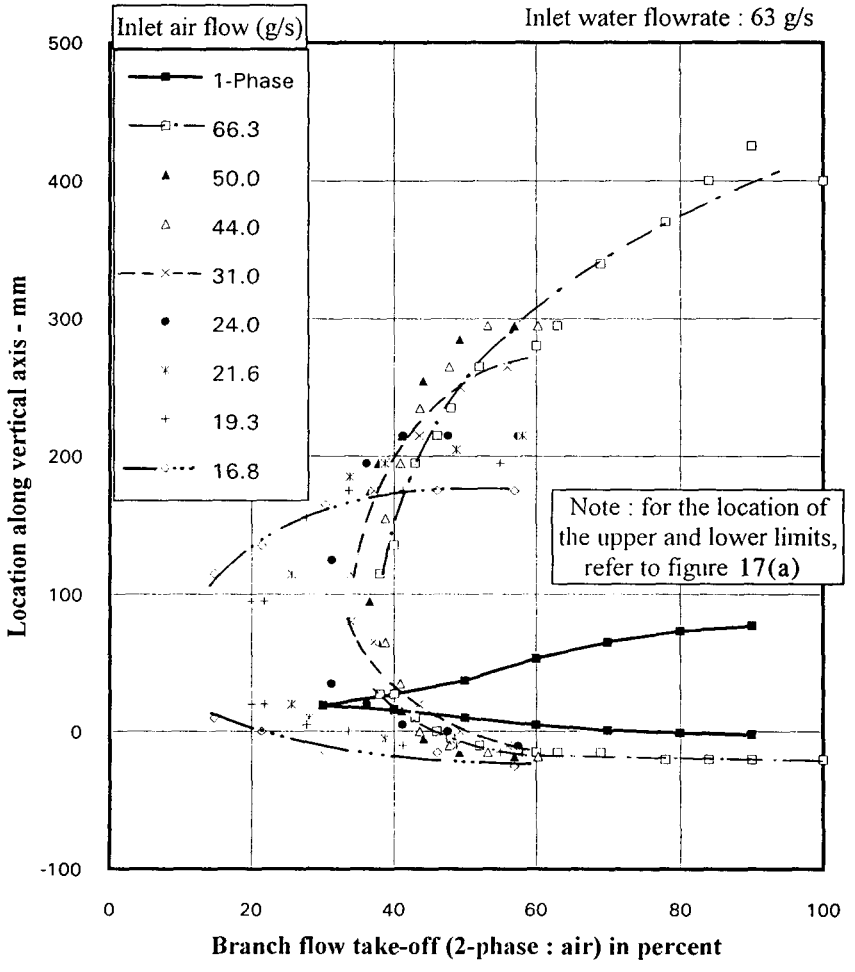

Figure 8. Upper and lower limits of flow circulation/reversal at run in single-phase and two-phase flow.

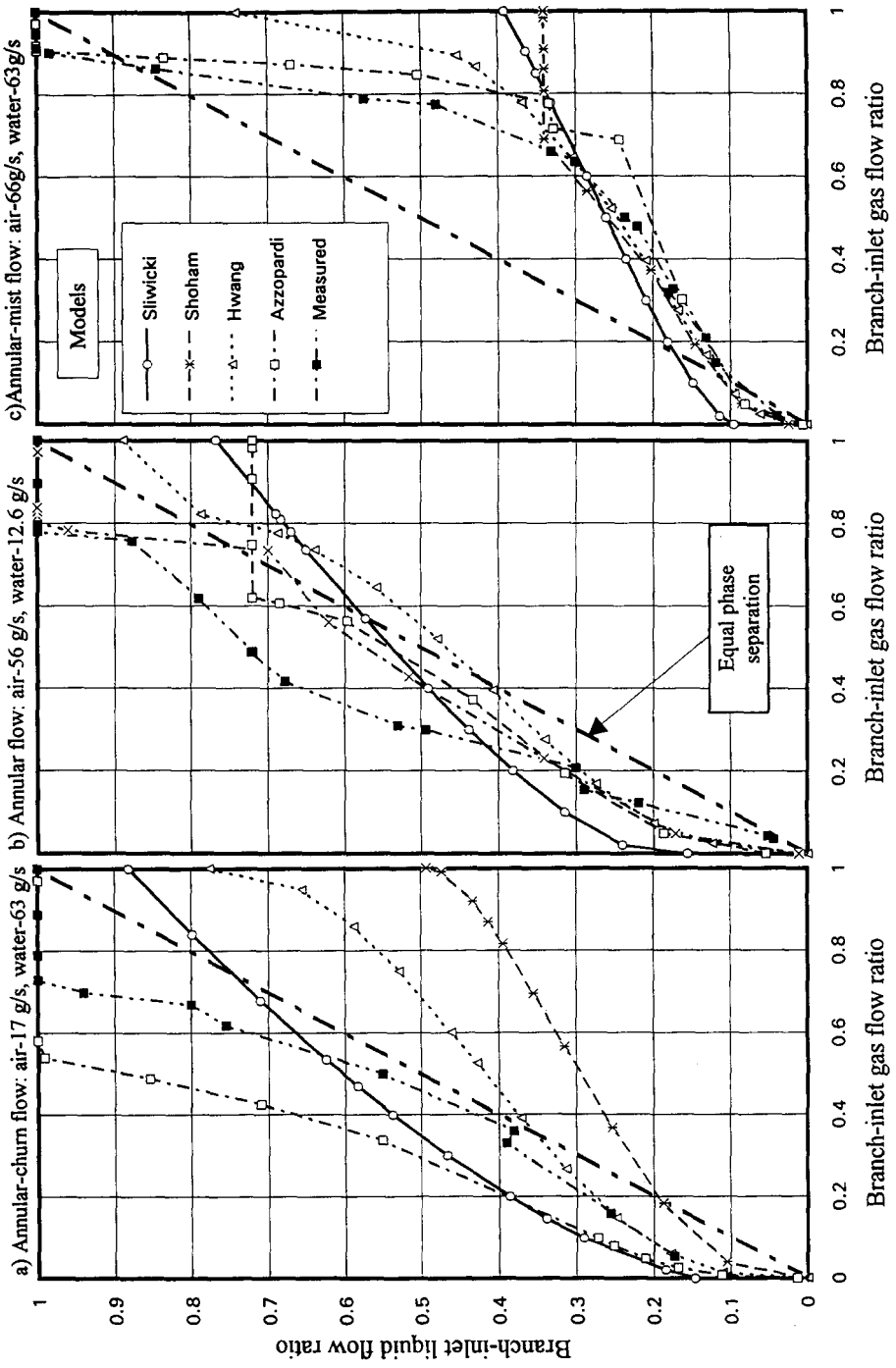

Figure 9. Liquid–gas flow split. Comparison between experimental data and predictions of several models.

deals with the specific case of vertical annular flow. Similarly, among the models proposed, only the model by Azzopardi covers the present application. Here, four models suitable for annular flow (three for horizontal flow) are tested against the present data.

The model designed by Hwang *et al.* (1988) is based on Euler equations, describing a particle trajectory in a curved path, and a number of assumptions: (a) accelerational forces are neglected; (b) some parameters in the streamline equations are determined empirically; (c) flows in the direction of the tee outlets come from inlet tee areas represented by circular segments; (d) in the case of a separated flow, the drag force is neglected, providing a simple relation between the gas and liquid centrifugal forces.

Shoham & Brill (1987) developed a model suitable for separated flows (stratified and annular flows). In this model the liquid movement is controlled by competing inertial, centrifugal and damping forces. For annular flow, the damping coefficient is an inverse square function of the film thickness.

In the model by Sliwicki & Mikielewicz (1988), two types of forces are considered for the liquid film entrainment to the branch: the surface tension and the gas drag forces. According to the authors, the effect of the first force would be very significant particularly at low gas branch take-off.

The model proposed by Azzopardi (1988) considers three types of liquid entrainment to the branch: (a) the liquid film taken-off from the segment where the gas is being removed, based on gas drag and relative momentum considerations; (b) an amplification of the liquid film entrainment when the liquid film stop phenomenon occurs, particularly noticeable when the inlet water flowrate is small; (c) in the case of a vertical outlet, the entrainment of all the liquid falling along the vertical outlet as a result of liquid flooding.

A comparison between the predictions of these models and the present measurements is provided in figure 9 for three typical flow conditions: (a) annular–churn, (b) annular and (c) annular–mist. These models provide generally satisfactory predictions. However, it should be noted that:

—only the model by Azzopardi considers the liquid flow reversal phenomenon. The other models are not designed for vertical tee junctions;
—the trend of the film stop phenomenon is relatively well represented by two models: those by Azzopardi (film stop calculated explicitly at certain conditions) and Shoham (film stop calculated implicitly at all flow conditions by means of the damping coefficient);
—the model by Sliwicki considerably over predicts the film entrainment at low take-off as a result of the surface tension force effect;
—the predictions by Hwang match the experimental data reasonably well. However, in many cases, this appears to be the result of an under prediction of the film flow take-off and an over prediction of the droplet flow take-off.

Performance of these models is surprisingly good considering that:

—the three-dimensional nature of the flow separation is not taken into account. References are made to the shape of the inlet gas velocity profile (section 2.1.1) and the shape of the dividing streamline boundary at the tee entrance (section 2.2). The liquid film drag is usually analysed in the symmetrical plane of the junction instead of the tube periphery. Mechanistic models are generally one-dimensionally based;
—rejection to the tee of a fraction of the liquid entering the branch is not taken into account (section 5.1);
—the secondary flow effect occurring at the tee entrance is not taken into account.

4. FLOW SEPARATION IN SINGLE-PHASE FLOW

At a cross section located at a short distance from the tee entrance (14 mm in figure 5) the dividing streamline boundary delimiting the flows in the two outlet directions presents a crescent shape, particularly noticeable when the flow take-off is not too high. The shape found can be

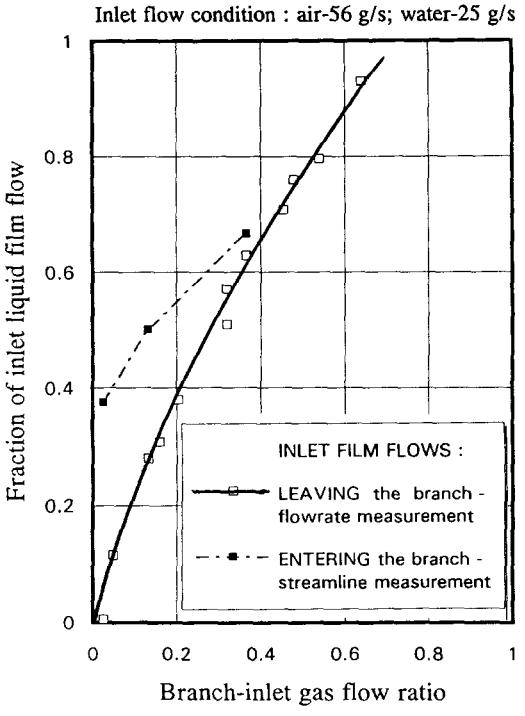

Figure 10. Comparison between mesured liquid film flows entering and leaving the branch.

explained by considering two effects: firstly, the velocity profile at the inlet, allowing the fluid travelling along the tube wall with low momentum to be more easily diverted to the side branch than the fast central fluid; secondly, the secondary flow which displaces the streamlines transversally according to their relative velocities and curvature radii.

Although the experiments could only be performed in single-phase flow, it seems reasonable to believe that in two-phase flow, the gas dividing streamlines would present the same type of shape characteristics, according to the previous explanation. The effect might be even greater, because of the more peaked velocity profiles (particularly in low quality flow). The shapes measured would therefore contradict the hypothesis currently made in two-phase separation models, that the gas entering the branch comes from a circular segment (section 3).

A second observation can be made about the relative sizes of the areas A_b and A_r representing the flows in the two outlet directions (branch and run, respectively). For intermediate gas branch take-off (F_G) values, A_b and A_r are approximately proportional to F_G and $1 - F_G$, however when F_G is small, A_b only decreases slowly. Considerations of velocity profiles and secondary flows at the tee entrance may only provide a partial answer to the variations observed. A third effect is proposed suggesting, that at low flow take-off, a fraction of the flow entering the branch would return to the junction after some circulation at the branch vena contracta. This hypothesis is substantiated at zero flow split:

(a) from pressure gradient consideration: slightly above the tee junction centre, the pressure reduces in the direction of the branch;
(b) from streamline visualization: cotton threads are oriented towards the run when they are located in the tee symmetrical plane and towards the branch at a few millimetres from this plane.

It is likely that this flow rejection phenomenon also occurs for positive branch take-off values, only disappearing when the driving force produced by the branch outlet flow is large enough to overcome the suctioning effect of the straight-through flow.

5. FLOW SEPARATION IN TWO-PHASE FLOW

5.1. Liquid film separation at the tee

A comparison between the liquid film flowrates entering and leaving the branch is shown in figure 10, in one typical flow case, indicating that as the branch flow take-off reduces the entering flowrate considerably exceeds the leaving flowrate. A scenario is proposed to explain this flow discrepancy: low momentum air streamlines at the gas–liquid interface and liquid film streamlines are progressively diverted towards the branch a few diameter lengths before the tee entrance, as shown by figure 11(a). These streamlines would mainly enter at the lateral sides of the branch as shown by figure 11(c). Inside the branch, the flow would divide in two parts [figure 11(b) and (d)], one continuing forward to the branch outlet and the other returning to the tee along the bottom of the branch tube. At the main-branch corner, the backward flow would be entrained towards the run by an ejection effect produced by the high momentum of the fluids flowing in the main-run direction, as shown by figure 11(b). This backward flow would be enhanced by the flow circulation occurring at the lower part of the branch entrance (branch vena contracta). This scenario is particularly well supported at zero branch outlet flow by the following observations:

—film streamlines (cotton threads) are oriented towards the branch [figures 11(a) and 7(a)];
—an annular flow is continuously formed at the branch entrance over a length of 2–5 times the tube diameter, depending on the inlet flow conditions [figures 11(a) and 7(a)];
—the liquid layer, at the bottom of the branch, flows back to the tee as seen during a dye test;
—from high speed video recordings, the rejected flow is not continuous but intermittent. The liquid rejection can also be observed *in situ*, as it takes the appearance of a relatively opaque cloud until it dilutes in the run line with the rest of the flow [figure 7(a) and (b)].

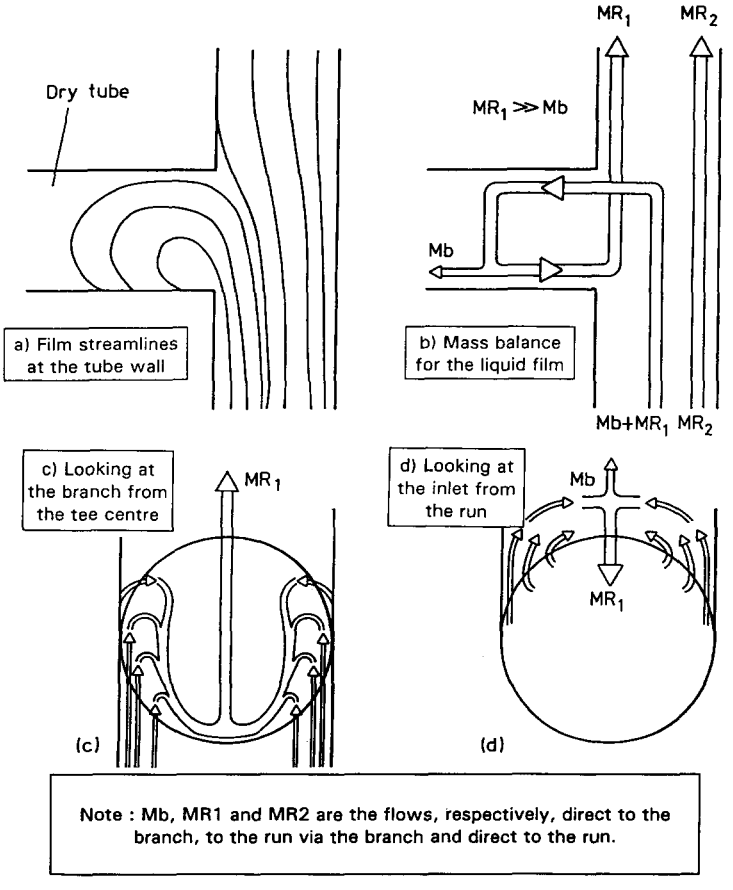

Figure 11. Liquid film behaviour at small branch take-off.

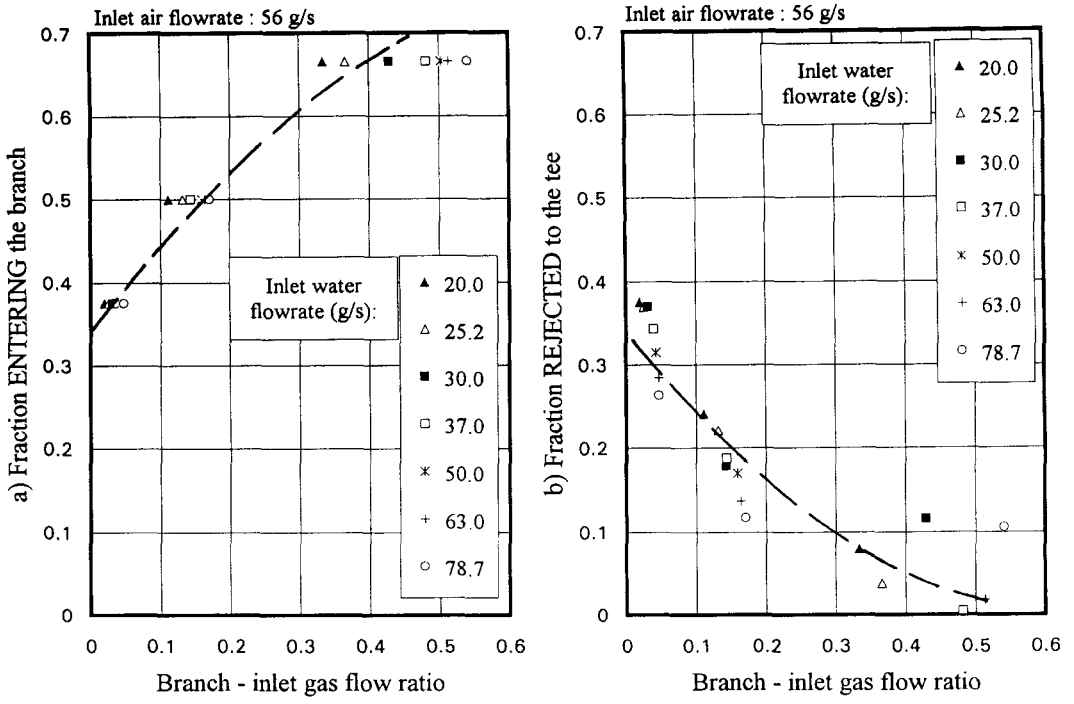

Figure 12. Fractions of inlet liquid film: entering the branch and rejected to the tee.

As the branch outlet flow becomes positive a horizontal drag force would be created, counteracting the vertical drag force and therefore limiting the rejection rate to the junction.

5.2. Branch liquid rejection to the tee

The fractions of the liquid film flow entering the branch and rejected to the tee have been measured for various inlet flow conditions. Some of the results are shown in figure 12(a) and (b) for constant inlet air flowrate. From these measurements it is found that:

—as the branch outlet flow increases, the amount of rejected liquid flow reduces. It falls to zero when the gas fraction leaving the branch reaches 30–50%, depending on the inlet flow conditions. The air fraction limit is relatively independent of the inlet water flowrate [figure 12(b)] but tends to reduce as the inlet air flowrate increases;

—at zero branch outlet flow, the fractions of inlet liquid film entering and leaving the branch are of the order of 30–35%, varying slightly with the inlet flow conditions.

The phenomenon of liquid flow rejection to the tee can also be analysed by plotting the rejected flowrate versus the inlet flow conditions, as shown by the figure 13, for constant inlet water flowrate. This figure indicates that the rejection rate varies approximately linearly with the inlet air flowrate. However, no clear conclusion could be drawn about the variation with the inlet water flowrate.

5.3. Liquid film stop

Azzopardi & Purvis (1987), considering the low inlet water flow case, noticed an important liquid film entrainment mechanism to the branch at low and medium flow splits which could not be predicted by his "segment" equation nor by the occurrence of flow reversal at the run. Azzopardi suggested that as the volume flowrate at the run reduces, the inlet flow kinetic energy is progressively converted to static pressure, creating a pressure rise at the tee vertical outlet and a deceleration of the inlet liquid film from the tee entrance. Above a certain flow split, a part or the entire film would be "stopped" at the tee and consequently easily removed by the branch.

The liquid film stop phenomenon is reviewed here in relation with the pressure measurements made in the close vicinity of the tee junction. In the vertical direction, the change in velocity resulting from the change in pressure can be written with Lagrangian co-ordinates as:

$$\frac{dU_{lfy}}{dt} = \frac{\tau_{iy}(r_i/r_o) - \tau_{wy}}{\rho_L m} - \frac{1}{\rho_L}\frac{dP}{dy} - g \qquad [4]$$

where τ_i, τ_w, r_i, r_o, dP/dy, g, ρ_L, U_{lf}, m, designate respectively the inner (interfacial) and outer (wall) shear forces and radii, the vertical pressure gradient, the gravitational acceleration, the liquid film density, velocity and thickness, while the subscript y indicates a vertical component.

The magnitude of the straight-through pressure gradient acting on the film is shown in figure 14, for several inlet water flowrate values (3.5–63 g/s), versus the gas branch take-off, F_G. The curves are based on pressure measurements taken at the tube wall, opposite the branch entrance, over a length of 0.6 tube diameter each side of the tee junction. The curves indicate hardly any difference in pressure gradient for $F_G < 0.3$, in the water flow range considered, whilst flow measurements at tee outlets do indicate very different liquid–gas flow separation when $F_G < 0.3$ [figure 6(a)].

The combined effect of the straight-through pressure gradient and the shear force acting on the film has been analysed in the same manner. The shear force data were calculated at the inlet tube, due to the lack of measurements at the tee junction itself. The combined force data again showed hardly any difference for $F_G < 0.3$, suggesting that another parameter must be considered to explain the liquid film separation phenomenon, at low inlet water flowrates.

The effect of the inlet liquid film velocity is examined in figure 15, in one case of gas branch take-off ($F_G = 32\%$), showing some correlation between the film velocity and the film flowrates entering and leaving the branch. A break point at 20 g/s, below which the film stop occurs, is particularly well represented by the three curves. The importance of the liquid film velocity could be anticipated from [4] acknowledging that the sum of the forces acting on the film varies very little with the inlet water flowrate, providing a constant film deceleration and consequently an earlier film stop to the slower inlet liquid film. Excluding the manner to determine the local pressure rise at the tee, the above is in accordance with Azzopardi analysis (1988).

5.4. Falling liquid phenomenon at the run

The falling liquid phenomenon at the run and the resulting liquid entrainment to the branch have been examined experimentally from dye tests and high speed videos, providing locations and conditions of occurrence for both phenomena.

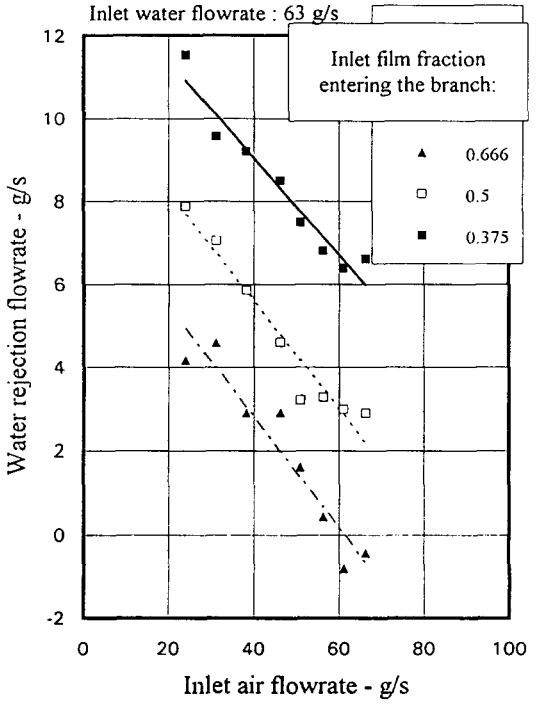

Figure 13. Liquid rejection from the branch for fixed fraction of inlet liquid film entering the branch.

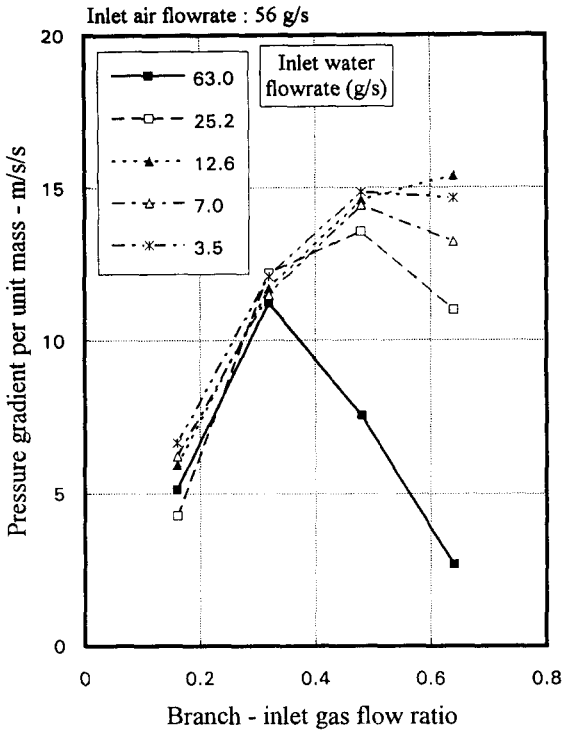

Figure 14. Pressure gradient per unit mass. Vertical direction, opposite side-branch.

5.4.1. Conditions of occurrence. Above 30 g/s inlet air flowrate, the falling liquid phenomenon occurs at a relatively constant gas branch take-off value of roughly 35%, a value also representative of the occurrence of a vena contracta in single-phase flow—figures 8 and 16, while below 30 g/s, the

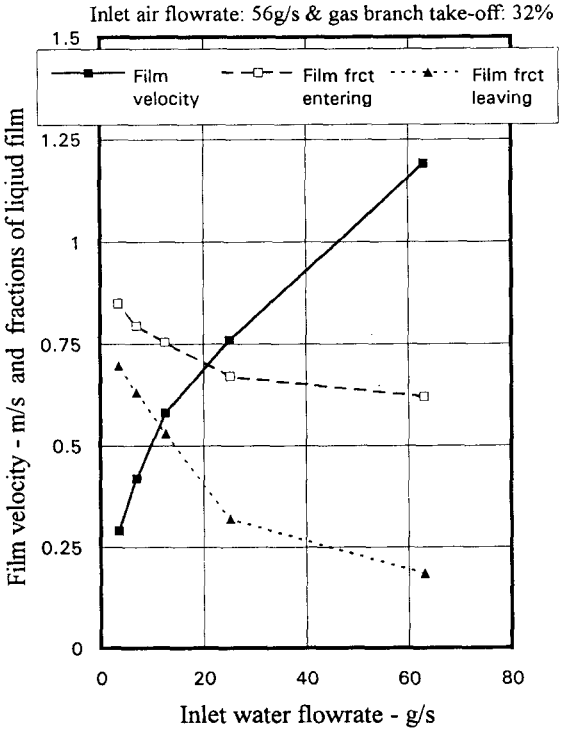

Figure 15. Inlet liquid film: velocity and fractions entering and leaving the branch.

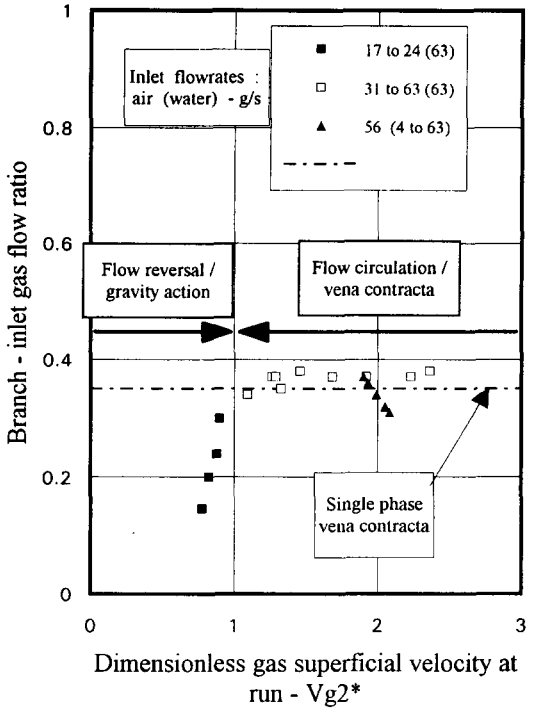

Figure 16. Onset of liquid falling at the vertical outlet in two-phase flow.

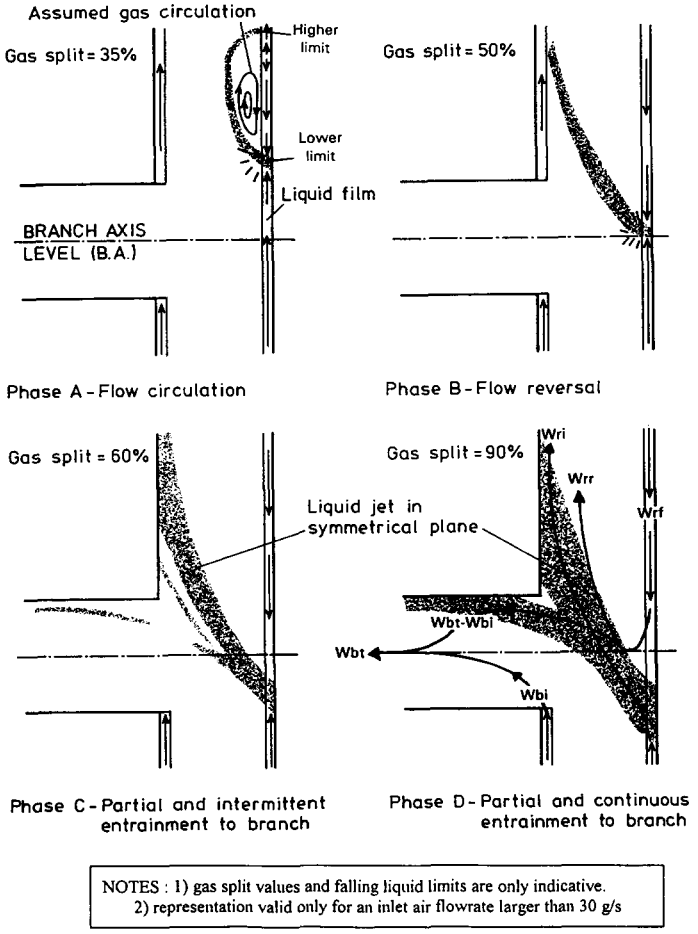

Figure 17. Schematic representation of four phases of the falling liquid at the tee vertical outlet.

corresponding value reduces as the inlet air flowrate reduces, keeping, however, the dimensionless gas superficial velocity at the run (defined in [7]) practically constant and equal to 1.

These observations lead us to believe that the liquid falls at the run, for one of the two following reasons, whichever occurs first: (a) vena contracta formation, above a certain flow split at the run, a phenomenon here called *flow circulation*, (b) gravity force action, below a certain dimensionless gas superficial velocity at the run, here called, *flow reversal*.

It should be noted that the measured branch–inlet flow ratio corresponding to the occurrence of the vena contracta in single-phase flow (30–35% here) is slightly lower than the value found by Hervieu (1988), 45%, possibly because our measurements were taken at a smaller distance from the tube wall (1 mm instead of 4 mm), allowing an earlier detection of the flow circulation at run.

5.4.2. Location. The liquid falling occurs opposite the branch over a distance considerably larger than for the vena contracta in single-phase flow.

—*Lower limit.* Below 30 g/s air flowrate, at the onset of the liquid falling, the lower limit sets approximately at the branch axis level, BA, whereas it is significantly higher with larger air flowrates (figure 17, phase A). Above 30 g/s, as F_G increases, the gravity force increases and the lower limit moves down towards the BA level (phase B). At all air flowrates, for further increase of F_G, the limit falls below the BA level towards the tee entrance level (phase C). This level is rarely exceeded, except for very low inlet air flowrates and high take-off, due to the action of the rising inlet flow provided with relatively high momentum (phase D).

—*Higher limit.* The figure 8 indicates that this limit varies with the inlet flowrates: the higher the inlet air or water flowrate, the higher the upper limit elevation. It varies also with F_G but in a more complex manner: successively increasing and decreasing with F_G.

5.5. Division of the falling liquid flow at the tee junction

As the liquid falls along the run, opposite the side branch, a liquid jet is formed at the impact between the falling and rising flows. The jet is subject to two competing forces: in the direction of the branch (pressure force) and in the direction of the run (inertial and drag forces), with magnitudes varying with F_G. Observations of the liquid jet, from high speed video recordings, indicate that the largest part of the liquid jet is directed towards the run whereas its entrainment

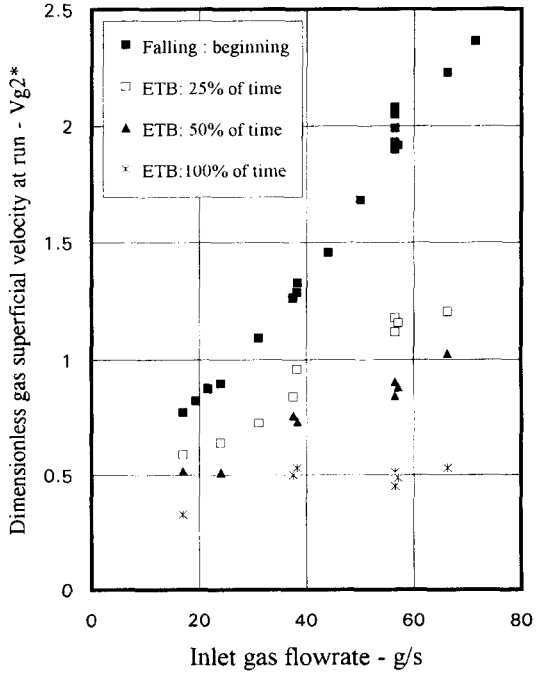

Figure 18. Falling liquid at run in two-phase flow and its Entrainment to Branch (ETB).

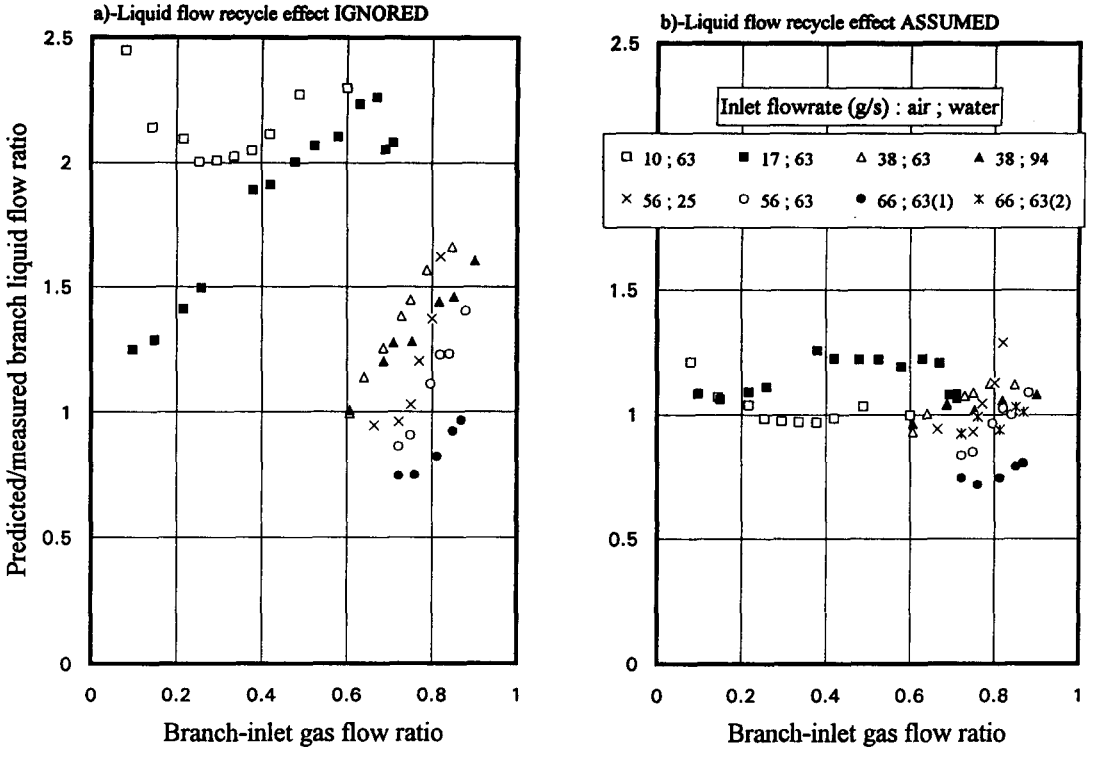

Figure 19. Liquid flow reversal and recycle at the tee vertical outlet.

to the branch (when it occurs), is intermittent, as shown by the two photographs (c) and (d) in figure 7, taken at the same flow conditions but at a 1 second interval. The intermittence effect is graphically represented in figure 18, where details concerning the fraction of time during which the falling liquid enters the branch are provided. It can be seen from this figure, that the beginning of the entrainment to the branch (close to ETB = 25%) occurs at a much lower dimensionless gas superficial velocity at the run [7] than for the onset of liquid falling at the run.

The division at the tee of the falling liquid flow can also be established by considering the amount of falling liquid flow re-injected into the run, W_{rr}. This parameter is related to the following liquid flowrates: (a) W_{bi}, film directly entrained from the inlet to the branch; (b) W_{bt}, actually leaving the branch outlet; (c) W_{rf}, falling along the run (figure 17, phase D); by:

$$W_{rr} = W_{rf} - (W_{bt} - W_{bi}) \quad [5]$$

W_{rf} can be calculated from a flooding correlation by Wallis (1961) or a liquid down flow correlation by Govan (1991), defined by:

$$\sqrt{V^*_{G2}} + \sqrt{V^*_{L2}} = C \quad [6]$$

where, according to Wallis, $C = 0.6$ to 1.0 depending on the mode of fluid entrance while, according to Govan, $C = 0.97$ (experiments carried out with air and water, at 1.33 bar, in a 31.75 mm diameter tube). The dimensionless superficial velocities at the run of the rising gas, V^*_{G2} and of the falling liquid, V^*_{L2} are defined by:

$$V^*_{i2} = V_{i2}(\rho_i/((\rho_L - \rho_G)gd_2))^{1/2} \quad [7]$$

where i = G (gas) or L (liquid), V_{i2} is a superficial velocity at the run and d_2 the run diameter.

Azzopardi assumed that when the flow reversal occurs, all the falling liquid flow is entrained towards the branch, i.e. $W_{rr} = 0$. This assumption is checked in figure 19(a) by comparing the measured values of W_{bt} with that predicted by [5] by making $W_{rr} = 0$. The calculation is done using Azzopardi data, i.e. $C = 0.88$ in [6] and with W_{bi} calculated from the "segment" equation (Azzopardi 1988). The discrepancies observed confirm the observations made from the high speed

videos, that is, the re-injection into the run of an important fraction of the falling liquid. Moreover, the figure indicates that the re-injected liquid fraction increases as the inlet gas flowrate reduces, while the effect of the inlet liquid flowrate is relatively less important (compare the inlet liquid flowrate effect at 56 g/s gas flowrate). From the trends shown by figure 19(a) an empirical law is proposed for the division at the tee junction of the falling liquid with the fraction to the branch:

$$F_B = (V^*_{Gl})^{n_r}/K_r \text{ or } 1 \text{ if numerator} > \text{denominator} \quad [8a]$$

and the fraction to the run:

$$F_R = 1 - F_B \quad [8b]$$

where V^*_{Gl} is the dimensionless gas superficial velocity at the inlet. The re-injection hypothesis is presented in figure 19(b) with $K_r = 2.5$ and $n_r = 0.5$, showing a considerable improvement in the representation of the division of the falling liquid. It can be noted that [8a] and [8b] are less satisfactory at the highest air flowrates. This problem could result from the choice of the parameter C as shown in figure 19(b) by the two sets of data 66–63 (1) with $C = 0.97$ and 66–63 (2) with $C = 1.08$.

6. CONCLUSION

The separation of the flow at a tee junction mounted vertically has been examined in single-phase and two-phase flows.

In single-phase flow, experiments have shown: firstly, that the dividing streamline boundary at a cross section presents a crescent shape with a concavity increasing as the branch flow take-off reduces, and secondly, at low take-off, that a fraction of the flow entering the branch is re-injected to the tee.

In two-phase flow, experiments were carried out to examine the separation of the inlet liquid film flow and the behaviour of the falling liquid flow at the vertical outlet:

—liquid film separation experiments have shown that there were considerable discrepancies between the liquid film flowrates entering the branch and actually leaving it, particularly at low take-off, caused, similarly to single-phase flow, by re-injection to the tee of a fraction of the entering flow. The phenomenon is more significant for the liquid film than for the gas, owing to their relative radial positions and therefore velocities. The fraction of the inlet film re-injected to the tee is of the order of 30% at zero branch take-off;

—the liquid film stop phenomenon was analysed in relation to the pressure change measurements made in the close vicinity of the junction. These data, varying very little in a wide band of inlet liquid flowrates, indicated that the liquid film was practically uniformly and constantly decelerated at constant gas branch take-off and consequently the inlet liquid film velocity is important in predicting the occurrence of the film stop;

—the falling liquid phenomenon at the vertical outlet and opposite the side-branch was interpreted as the result of: either the formation of a vena contracta above a certain gas branch take-off or the occurrence of liquid flooding at the vertical outlet. In the second case, the length of the falling region is considerably longer than the length of the vena contracta obtained in single-phase and in two-phase flows (ratio of 5:1 or more). At the impact between the falling and rising liquid flows, a liquid jet is formed, directed upwards. Calculations and video recordings have shown that not all the falling liquid is entrained to the side-branch but only a fraction of it, varying with the gas branch take-off.

The present two-phase flow separation measurements were satisfactorily predicted by models from Shoham, Hwang and Azzopardi outside the cases of liquid film stop (not covered by Hwang's model) and liquid flow reversal (not covered by Shoham's nor Hwang's models). The relatively good predictions of some mechanically-based models is nevertheless surprising, considering that several flow separation features observed during the present experiments are not, or are wrongly taken into account by these models. Examples are: the branch liquid flow rejection to the junction, the shape of the gas dividing streamline boundary, the deflection of the flow streamlines upstream the tee entrance, the radial velocity profiles at inlet. It is questionable whether these models would be as satisfactory with different conditions of fluids or flows.

Acknowledgement—The work described in this paper was supported by the programme of Corporate Investment Research of AEA Technology at Harwell, Oxfordshire, England. Published with permission from AEA Technology.

REFERENCES

Adorni, N. 1961 Phase and velocity distribution measurements in a round vertical tube. CISE R-91.

Azzopardi, B. J. 1984 the effect of the side arm diameter on the two-phase flow split at a tee junction. *Int. J. Multiphase Flow* **10,** 509–512.

Azzopardi, B. J. 1988 An additional mechanism in the flow split of high quality gas–liquid flows at a tee junction. AERE-R 13058.

Azzopardi, B. J. & Hervieu, E. 1992 Phase separation at a tee junction. *3rd Int. Workshop on Two-phase Flow Fundamentals*, Imperial College, London.

Azzopardi, B. J. & Purvis, A. 1987 Measurements of the split of a two-phase flow at a vertical tee junction. AERE-R 12441.

Azzopardi, B. J. & Whalley, P. B. 1982 The effect of flow patterns on two-phase flow in a tee junction. *Int. J. Multiphase Flow* **8,** 491–507.

Ballyk, J. D. & Shoukri, M. 1990 On the development of a model for predicting phase separation phenomena in dividing two-phase flow. *Nucl. Engng Design* **123,** 67–75.

Charron, Y. 1993 Two-phase flow in a vertical tee junction. D.Phil. Thesis, University of Oxford.

Gill, L. F., Hewitt, G. F. & Lacey, P. M. C. 1963 Sampling probe studies of the gas core in annular two-phase flow; Part II. *Chem. Engng Sci.* **19,** 665–682.

Govan, A. H., Hewitt, G. F. & Richter, H. J. 1991 Flooding and churn flow in vertical pipes. *Int. J. Multiphase Flow* **17,** 27–44.

Hervieu, E. 1988 Ecoulement monophasique et diphasique à bulles dans un branchement en té. Thèse de docteur de l'INPG.

Hong, K. C. 1978 Two-phase flow splitting in a pipe tee. *J. Pet. Technol.* 290–296.

Hwang, S. T., Soliman, H. M. & Lahey, R. T. 1988 Phase separation in dividing two-phase flows. *Int. J. Multiphase Flow* **14,** 439–458.

Maciaszek, T. & Micaelli, J. C. 1988 A phase separation model for tee junctions application to a PWR code safety code. *25th Natn. Heat Transfer Conf.*, Houston, TX, Vol. 3, pp. 82–89.

McCreery, G. E. & Banerjee, S. 1990 Phase separation of dispersed mist and dispersed annular flow in a tee—part I. *Int. J. Multiphase Flow* **16,** 429–445.

McNown, J. S. 1954 Mechanics of manifold flow. *Am. Soc. Civ. Engrs* **119,** 1103–1142.

Rao, C. S. & Dukler, A. E. 1971 The isokinetic-momentum probe. A new technique for measurement of local voids and velocities in flow of dispersions. *Ind. Engng Chem. Fundam.* **10,** No. 3.

Reimann, J., Brinkmann, H. J. & Domanski, R. 1988 Gas–liquid flow in dividing tee-junctions with a horizontal inlet and different branch orientations. KFK 4399.

Schraub, F. A. 1966 Isokinetic sampling probe technique applied to two-phase flow. GEAP 5287, AEC R&D report.

Shoham, O. & Brill, J. P. 1987 Two-phase flow splitting in a tee junction. Experiment and modelling. *Chem. Engng Sci.* **12,** 2667–2676.

Sliwicki, E. & Mikielewicz, J. 1988 Analysis of an annular-mist flow model in a tee junction. *Int. J. Multiphase Flow* **14,** 321–331.

Teixeira, J. C. F. 1988 Turbulence in annular two-phase flow. Ph.D. thesis, University of Birmingham.

Wallis, G. B. 1961 Flooding velocities for air and water in vertical tubes. UKAEA report, AEEW R123.

Zetzmann, K. 1982 Phase separation and pressure drop in two-phase flow through vertical tee junction. Doktor Ingenieur Dissertation, Universitat Hannover.